Orbital control on exceptional fossil preservation

Farid Saleh, Bernard Pittet, Jean-Philippe Perrillat, Bertrand Lefebvre

Publisher: GSA
Journal: GEOL: Geology
DOI:10.1130/G45598.1

Orbital control on exceptional fossil preservation

Farid Saleh*, Bernard Pittet*, Jean-Philippe Perrillat*, and Bertrand Lefebvre*

Univ. Lyon, Université Claude Bernard Lyon 1, ENS de Lyon, CNRS, UMR 5276 Laboratoire de Géologie de Lyon: Terre, Planètes, Environnement, F-69622 Villeurbanne, France

*E-mails: farid.saleh@univ-lyon1.fr; bernard.pittet@univ-lyon1.fr; jean-philippe.perrillat@univ-lyon1.fr; bertrand.lefebvre@univ-lyon1.fr

ABSTRACT

Exceptional preservation is defined by the preservation of soft to lightly sclerotized organic tissues. The two most abundant types of soft tissues preservation are carbonaceous compressions and replicates in authigenic minerals. In the geological record, exceptionally preserved soft fossils are rare and generally limited to only a few stratigraphic intervals. In the Fezouata Shale (Lower Ordovician), we found that deposits yielding pyritized soft tissues contain iron-rich silicate minerals. These minerals played a crucial role in inhibiting decaying bacteria and are comparable to those found in formations yielding carbonaceous soft parts around the world. Furthermore, we found that iron-rich minerals show a cyclic pattern of occurrence (of ~100 kyrs periodicity) implicating a short eccentricity control through the general oceanic and atmospheric circulations on iron availability. Our results identify, for the first time, an external climate forcing on exceptional preservation and show that orbital forcing may be a level-selective parameter responsible for the discontinuous occurrence of horizons preserving soft parts around the world.

INTRODUCTION

Exceptional preservation consists of the preservation of soft to lightly sclerotized organic tissues (e.g., feathers, guts, skins) in the geological record (Butterfield, 1995). The transfer of such tissues from the biosphere to the lithosphere is the result of a succession of multiple, complex biological and geological mechanisms. Deciphering these mechanisms is essential to understanding why exceptional preservation is limited to specific intervals in the sedimentary record. Recent studies have shown that the absence/presence of carbonaceous soft tissues is strongly correlated with the mineralogy of the depositional environment and most importantly with iron-rich minerals that can inhibit bacterial decay of soft tissues through the oxidative damage of bacterial cells (McMahon et al., 2016; Anderson et al., 2018). However, little attention has been paid so far to discover within which sediment minerals the pyritized soft tissues occur and what are the processes behind the deposition of these minerals.

The Fezouata Shale crops out in the Zagora region in southern Morocco. This Lower Ordovician succession consists of blue-green to yellow-green sandy mudstones and siltstones that coarsen upwards. These sediments are up to 900 m thick in the Zagora region (Destombes et al., 1985; Martin et al., 2016; Vaucher et al., 2017). The entire succession was deposited in a marginal basin at high latitude close to the paleo-South pole (Torsvik and Cocks, 2011, 2013). The shallow depositional setting ranges from the foreshore to the upper offshore. It was storm-wave dominated (Martin et al., 2016) and indirectly influenced by tides (Vaucher et al., 2017). The Fezouata Shale has yielded abundant remains of soft-bodied organisms preserved with high fidelity, showing the association of post-Cambrian taxa typical of the Great Ordovician Biodiversification Event along with iconic taxa of the Cambrian Explosion (Van Roy et al., 2010, 2015).

Most soft bodied organisms were pyritized and are now preserved in iron oxides. However, this weathering impact is not substantial as numerous fossils still show original framboidal pyrite crystals. The presence of levels yielding both mineralized and soft bodied organisms, as well as the highly constrained stratigraphic framework of this formation (Gutiérrez-Marco and Martin, 2016; Lehnert et al., 2016; Martin et al., 2016; Nowak et al., 2016; Lefebvre et al., 2018), make the Fezouata Shale a good candidate to investigate whether specific sediment minerals are correlated with pyritized soft parts, and if these mineralogical signatures change through time.

MATERIAL AND METHODS

Mineralogical Signatures

Part of the sedimentary succession of the Fezouata Shale (Vaucher et al. 2016) was included in this study. The mineralogy of all fossiliferous levels in this section was investigated. Mineral assemblages of levels yielding exceptional preservation were compared to those in levels bearing only sclerotized remains. Matrix samples from each level were prepared as randomly orientated powdered aggregates (< 10 μm), without any specific treatments, on thermoplastic polymer (PMMA) substrates. X-ray diffraction (XRD) was performed using a Bruker D8 Advance diffractometer, employing a CuKα source and Bruker LynxeyeX detector. Peak positions were adjusted for slight variations in sample height displacement error using positions of quartz peaks as internal standards. Mineral phases were then retrieved based on indexation of their diffraction lines, between 0 and 75° 2θ values, from the ICDD (International Centre for Diffraction Data) PDF4+ 2016 reference database. Illite is generally characterized by its basal (001) peak at ~10 Å. Quartz is characterized by its intense (011) reflection at 3.34 Å. The differentiation between chlorite minerals is verified based on the lateral variations of their characteristic (001) and (002) peaks, respectively at 14 and 7 Å, as iron enrichment causes an increase in d-spacing that shifts peaks positions toward higher 2θ values (Fig. 1). Phase proportions were estimated from the relative intensity of diffraction lines of each mineral species.

Sequence Reconstructions

The depositional environment of the Fezouata Shale is storm/wave dominated and indirectly influenced by tides (Martin et al. 2016; Vaucher et al., 2016, 2017). In the Fezouata Shale, the interaction of oscillations with surface sediments generated oscillatory structures. The wavelength of these structures decreased from shallow to deep environments (Nichols, 2010; Vaucher et al. 2016). Additionally, coarser sediments indicate a shallower environment, while finer sediments are deposited in deeper settings (Vaucher et al., 2016, 2017). These sediments and structural heterogeneities permitted the establishment of a model of facies for the Fezouata Shale (Vaucher et al. 2017). Based on this model, the alternation of deeper and shallower facies F1, F2 and F4 of Vaucher et al. (2017) allowed us to identify small-, medium- and large-scale sequences. Small-scale sequences correspond to the shortest variations of the sea level (Fig. 2), whereas medium- and large-scale sequences correspond to longer terms sea-level changes.

Bathymetry and Oxygenation

The depth of the water column was estimated accordingly with medium-scale sea level sequences (Lefebvre et al., 2016; Vaucher et al., 2017). Relative oxygen abundances in superficial sediments was reconstructed based on depth variations of the water column. In the Fezouata environment, in deep environments, in shelf settings

Publisher: GSA
Journal: GEOL: Geology
DOI:10.1130/G45598.1

below storm wave base, rapid burial did not occur, inhibiting the establishment of anoxic conditions in surface sediments (Vaucher et al., 2017). Above storm wave base, where rapid burial during storm events occurred, the establishment of anoxic conditions in surface sediments below the storm deposits was influenced by wave/sediment interactions. Wave/sediment interactions are more pronounced in shallow-most settings (Nichols, 2010), leading to an increase in the oxygen penetration depth from the water column to the sediments (Chatelain and Guizien, 2010). Thus, anoxic/dysoxic conditions occur rarely in the shallowest environments (decimetric wavelength of storm oscillatory structures, high oxygen penetration depth) and may occur only in less shallow deposits (centimetric wavelength of storm structures, limited oxygen penetration depth) just above the storm wave base (Fig. 2) in the Fezouata Shale (Vaucher et al. 2016., 2017).

RESULTS

All samples show a similar composition with an absence of organic matter, a high abundance of illite $(K,H_3O)(Al,Mg,Fe)_2(Si,Al)_4O_{10}[(OH)_2,(H_2O)]$ (~60%) and quartz SiO_2 (~30%), and a small portion (<10%) of chlorite minerals (see Table DR1 in the Data Repository for precise percentages). However, the nature of the chlorite phase differs between samples as some specimens show the presence of clinochlore $(Mg_5Al)(AlSi_3)O_{10}(OH)_8$, while others show iron-rich clinochlore $(Mg,Fe)_5Al(Si_3Al)O_{10}(OH)_8$ (iron content ~12%) or chamosite $(Fe_5Al)(AlSi_3)O_{10}(OH)_8$ (iron content ~30%) (Fig. 2). In the Fezouata Shale, the occurrence of soft tissues is discontinuous and is limited only to few stratigraphic levels in interval 1 (Fig. 2).

The entire sedimentary succession was deposited around the storm wave base. Both intervals 1 and 3 (Fig. 2), were deposited under anoxic/dysoxic conditions. The largest part of interval 2 was deposited under oxic conditions (Fig. 2).

The studied section contains ~2 medium-scale and 9 small-scale sequences. The occurrence of 4 small-scale sequences per medium-scale sequence deduced from facies changes (Fig. 2) in the entire sedimentary succession suggests an eccentricity control on sequence formation through its 100 and 400 kyrs periodicities. The studied sediments were deposited during the Tremadocian (duration of 7.7 ± 3.3 Ma). In the Tremadocian, 10 main graptolites subdivisions (biozones) of ~0,7 Ma have been identified (Loydell, 2012). In the Fezouata Shale, the first three biozones of the Tremadocian are missing (Gutiérrez-Marco and Martin, 2016; Lefebvre et al., 2018). This suggests that the Tremadocian sediments (450 m) of the Fezouata Shale were deposited over 5.7 ± 2.4 Ma. In addition, the sedimentation of the Fezouata Shale appears to be uniform (i.e., monotonous sequence dominated by siltstones) and formed by the stacking of storm deposits (mm- to cm-thick sandstone or coarse siltstone levels separated by mm-thick argillaceous siltstone or fine-grained siltstone layers) (Vaucher et al., 2016, 2017). This homogeneity of the sediments and the absence of observed long or short-term sedimentary hiatus (Vaucher et al., 2017) both suggest a relatively stable accumulation rate of ~79 m/Ma. Thus, the studied 67 m-thick section was deposited over ~0.84 ± 0.35 Ma. One medium-scale sequence would then represent a time interval of ~0.42 ± 0.17 Ma, and one small-scale sequence of 0.09 ± 0.03 Ma. These estimated durations are in accordance with the durations of eccentricity cycles.

DISCUSSION

Publisher: GSA
Journal: GEOL: Geology
DOI:10.1130/G45598.1

The sediment in the Fezouata Shale has a relatively simple composition comparable to other Paleozoic sites with exceptional preservation (Anderson et al., 2018). In this formation, chamosite appears to be correlated with levels recording exceptional preservation (Fig. 2). Chamosite can be formed directly from the transformation of primary clay minerals (kaolinite, glauconite) at high temperatures (T>175 °C) or from the transformation of berthierine, an iron rich serpentine phyllosilicate, in less extreme conditions (T<100 °C; Tang et al., 2017). In the Fezouata Shale, sediments did not endure extreme temperatures and burial conditions, and only 2–3 km (i.e., equivalent of burial temperatures between 70 and 100 °C using a mean geothermal gradient of 30° per km in passive margins) of sediments were deposited over these shales (Ruiz et al., 2008). Thus, berthierine is the most probable precursor for chamosite in the Fezouata Shale. In addition to that, chamosite occurrences appear to be correlated with an intermediate bathymetry, as it occurs only in intervals 1 and 3 (Fig. 2). In the Fezouata Shale, specific parameters (e.g. bathymetry, oxygenation) controlled the precipitation of berthierine in the depositional environment and were thus indirectly responsible of the selective presence of chamosite.

In a depositional environment, the presence of a significant amount of iron under reducing conditions leads to the precipitation of berthierine (Tang et al., 2017), a mineral which can inhibit decay bacteria (McMahon et al., 2016). Afterward, during a deeper burial, most of the berthierine is transformed to chamosite (Hornibrook and Longstaffe, 1996). In some levels of intervals 1 and 3, reducing conditions and abundant iron were available, leading to berthierine precipitation in sediments in addition to the pyritization of decaying soft parts. In interval 1, some levels, deposited under similar bathymetry (i.e., fast burial and sedimentary anoxia), yield mostly clinochlore instead of chamosite. Clinochlore and chamosite belong to the same chlorite mineral group, and lie on its magnesium-rich and iron-rich poles respectively (Curtis et al., 1985). The occurrence of both chamosite and clinochlore in intervals with different porosities suggests that the formation of these minerals is independent from the physical parameters in the sediments. Instead, the presence of clinochlore is likely related to iron deficiencies in these levels during early diagenesis.

In interval 2, chamosite is absent, and was mainly replaced by iron rich clinochlore indicating the presence of iron. The absence of chamosite and exceptional preservation in this interval were due to the absence of favorable reducing conditions (Fig. 2).

Iron, an important element for the formation of both berthierine and pyrite, may have different sources such as (i) circulation of iron-rich hydrothermal fluids (Tang et al., 2017), (ii) microbial extraction of iron from clay minerals after their deposition in marine sediments (Vorhies and Gaines, 2009) or (iii) iron inputs to the sea from other marine or continental sources (Odin and Matter, 1981). In the Fezouata Shale, illite, which is the main clay mineral in sedimentary basins (Ruiz et al. 2008), is present in all intervals. However, chamosite does not occur in all levels showing a different distribution than illite. This implies that the scenario considering microbial iron extraction from clay minerals is not parsimonious. In addition, the occurrence of chamosite at the end of a regression/ beginning of a transgression of a small-scale sequence (Fig. 2) rules out hydrothermal fluids as the main source of iron and favors marine and/or continental inputs. The Fezouata Shale was deposited in a shallow sea near the South Pole with a limited oceanic circulation (Martin et al., 2016, Vaucher et al., 2017). Thus, the enrichment of iron is considered as continental in origin.

According to duration estimations based on graptolite biostratigraphy, any two consecutive iron rich intervals in interval 1 were deposited with an average delay of ~100 kyrs in pace with eccentricity-controlled sea-level cycles (Fig. 2). Astronomic calculations confirmed that even if the periodicity of the obliquity and precession decreased with time, eccentricity frequency was stable over the last 500 million years (Berger et al., 1992). These calculations were validated through robust responses of different sedimentary systems to astronomically controlled climate forcing from recent times to the Cambrian (Osleger and Read, 1991). Every 100 kyrs, eccentricity transitions from a circular to an elliptic orbit, or vice versa, influencing precession and thus, insolation and seasonal variations (Fig. 3). Consequently, these variations influence the evaporation/precipitation cycle, ice volume (Rampino, 1979), if any, as well as river fluxes and continental weathering (Horton et al., 2012), and thus the inputs of iron to the sea (Fig. 3). These inputs constitute a major contributor to iron abundances in oceans (Elrod et al., 2004), and lead to berthierine formation in shallow environments at the water/sediment interface (Odin and Gupta, 1988; Kozłowska and Maliszewska, 2015) when anoxic conditions are present (Tang et al. 2010).

For the first time, our results (1) provide detailed information on the mineralogical context in which pyritized soft tissues occur, (2) identify a temporal variation of minerals in a sedimentary succession with soft tissue preservation, and (3) evidence an orbital control on soft tissue fossilization. This external climate forcing may be responsible for the discontinuous occurrence of soft tissues in numerous formations around the world in which iron discrepancies between levels yielding exceptional preservation and those with only skeletal remains are evidenced (Anderson et al., 2018).

ACKNOWLEDGMENTS

This paper is a contribution to the TelluS-INTERRVIE project 'Mécanismes de préservation exceptionnelle dans la Formation des Fezouata', funded by the INSU, CNRS. The authors thank Pierre Sansjofre and Muriel Vidal for assistance during field work in Morocco, Guillaume Suan and Vincent Perrier for their advices, and Ruben Vera for assistance in XRD preparation. Three reviewers are also thanked for their helpful and constructive remarks.

REFERENCES CITED

Anderson, R.P., Tosca, N.J., Gaines, R.R., Mongiardino Koch, N., and Briggs, D.E., 2018, A mineralogical signature for Burgess Shale–type fossilization: Geology, v. 46, p. 347–350, https://doi.org/10.1130/G39941.1.

Berger, A., Loutre, M.F., and Laskar, J., 1992, Stability of the astronomical frequencies over the Earth's history for paleoclimate studies: Science, v. 255, p. 560–566, https://doi.org/10.1126/science.255.5044.560.

Butterfield, N.J., 1995, Secular distribution of Burgess-Shale-type preservation: Lethaia, v. 28, p. 1–13, https://doi.org/10.1111/j.1502-3931.1995.tb01587.x.

Chatelain, M., and Guizien, K., 2010, Modelling coupled turbulence–dissolved oxygen dynamics near the sediment–water interface under wind waves and sea swell: Water Research, v. 44, p. 1361–1372, https://doi.org/10.1016/j.watres.2009.11.010.

Curtis, C.D., Hughes, C.R., Whiteman, J.A., and Whittle, C.K., 1985, Compositional variation within some sedimentary chlorites and some comments on their origin:

Publisher: GSA
Journal: GEOL: Geology
DOI:10.1130/G45598.1

Mineralogical Magazine, v. 49, p. 375–386, https://doi.org/10.1180/minmag.1985.049.352.08.

Destombes, J., Hollard, H., and Willefert, S., 1985, Lower Palaeozoic rocks of Morocco, *in* Holland, C.H., ed., Lower Palaeozoic Rocks of the World, volume 4: Lower Palaeozoic rocks of Northwest and West-Central Africa: Chichester, UK, John Wiley and Sons, p. 91–336.

Elrod, V.A., Berelson, W.M., Coale, K.H., and Johnson, K.S., 2004, The flux of iron from continental shelf sediments: A missing source for global budgets: Geophysical Research Letters, v. 31, L12307, https://doi.org/10.1029/2004GL020216.

Gutiérrez-Marco, J.C., and Martin, E.L.O., 2016, Biostratigraphy and palaeoecology of Lower Ordovician graptolites from the Fezouata Shale (Moroccan Anti-Atlas): Palaeogeography, Palaeoclimatology, Palaeoecology, v. 460, p. 35–49, https://doi.org/10.1016/j.palaeo.2016.07.026.

Hornibrook, E.R.C., and Longstaffe, F.J., 1996, Berthierine from the Lower Cretaceous Clearwater Formation, Alberta, Canada: Clays and Clay Minerals, v. 44, p. 1–21, https://doi.org/10.1346/CCMN.1996.0440101.

Horton, D.E., Poulsen, C.J., Montañez, I.P., and DiMichele, W.A., 2012, Eccentricity-paced late Paleozoic climate change: Palaeogeography, Palaeoclimatology, Palaeoecology, v. 331–332, p. 150–161, https://doi.org/10.1016/j.palaeo.2012.03.014.

Kozłowska, A., and Maliszewska, A., 2015, Berthierine in the Middle Jurassic sideritic rocks from southern Poland: Geological Quarterly, v. 59, p. 551–564.

Lefebvre, B., et al., 2016, Palaeoecological aspects of the diversification of echinoderms in the Lower Ordovician of central Anti-Atlas, Morocco: Palaeogeography, Palaeoclimatology, Palaeoecology, v. 460, p. 97–121, https://doi.org/10.1016/j.palaeo.2016.02.039.

Lefebvre, B., Gutiérrez-Marco, J.C., Lehnert, O., Martin, E.L.O., Nowak, H., Akodad, M., El Hariri, K., and Servais, T., 2018, Age calibration of the Lower Ordovician Fezouata Lagerstätte, Morocco: Lethaia, v. 51, p. 296–311, https://doi.org/10.1111/let.12240.

Lehnert, O., Nowak, H., Sarmiento, G.N., Gutiérrez-Marco, J.C., Akodad, M., and Servais, T., 2016, Conodonts from the Lower Ordovician of Morocco – contributions to age and faunal diversity of the Fezouata Lagerstätte and peri-Gondwana biogeography: Palaeogeography, Palaeoclimatology, Palaeoecology, v. 460, p. 50–61, https://doi.org/10.1016/j.palaeo.2016.03.023.

Loydell, D.K., 2012, Graptolite biozone correlation charts: Geological Magazine, v. 149, p. 124–132, https://doi.org/10.1017/S0016756811000513.

Martin, E.L.O., et al., 2016, The Lower Ordovician Fezouata Konservat-Lagerstätte from Morocco: Age, environment and evolutionary perspectives: Gondwana Research, v. 34, p. 274–283, https://doi.org/10.1016/j.gr.2015.03.009.

McMahon, S., Anderson, R.P., Saupe, E.E., and Briggs, D.E., 2016, Experimental evidence that clay inhibits bacterial decomposers: Implications for preservation of organic fossils: Geology, v. 44, p. 867–870, https://doi.org/10.1130/G38454.1.

Nichols, G., 2010, Sedimentology and Stratigraphy: Chichester, UK, Wiley-Blackwell, 432 p.

Nowak, H., Servais, T., Pittet, B., Vaucher, R., Akodad, M., Gaines, R.R., and Vandenbroucke, T.R., 2016, Palynomorphs of the Fezouata Shale (Lower Ordovician, Morocco): Age and environmental constraints of the Fezouata Biota: Palaeogeography, Palaeoclimatology, Palaeoecology, v. 460, p. 62–74, https://doi.org/10.1016/j.palaeo.2016.03.007.

Odin, G.S., and Gupta, B.K.S., 1988, Geological Significance of the Verdine Facies: Developments in Sedimentology, v. 45, p. 205–219, https://doi.org/10.1016/S0070-4571(08)70064-5.

Odin, G.S., and Matter, A., 1981, De glauconiarum origine: Sedimentology, v. 28, p. 611–641, https://doi.org/10.1111/j.1365-3091.1981.tb01925.x.

Osleger, D., and Read, J.F., 1991, Relation of eustasy to stacking patterns of meter-scale carbonate cycles, Late Cambrian, USA: Journal of Sedimentary Research, v. 61, p. 1225–1252.

Rampino, M.R., 1979, Possible relationships between changes in global ice volume, geomagnetic excursions, and the eccentricity of the Earth’s orbit: Geology, v. 7, p. 584–587, https://doi.org/10.1130/0091-7613(1979)7<584:PRBCIG>2.0.CO;2.

Ruiz, G., Helg, U., Negro, F., Adatte, T., and Burkhard, M., 2008, Illite crystallinity patterns in the Anti-Atlas of Morocco: Swiss Journal of Geosciences, v. 101, p. 387–395, https://doi.org/10.1007/s00015-008-1267-z.

Tang, D., Shi, X., Jiang, G., Zhou, X., and Shi, Q., 2017, Ferruginous seawater facilitates the transformation of glauconite to chamosite: An example from the Mesoproterozoic Xiamaling Formation of North China: American Mineralogist, v. 102, p. 2317–2332, https://doi.org/10.2138/am-2017-6136.

Torsvik, T.H., and Cocks, L.R.M., 2011, The Palaeozoic palaeogeography of central Gondwana: Geological Society of London, Special Publications, v. 357, p. 137–166, https://doi.org/10.1144/SP357.8.

Torsvik, T.H., and Cocks, L.R.M., 2013, New global palaeogeographical reconstructions for the Early Palaeozoic and their generation: Geological Society, London, Memoir 38, p. 5–24.

Van Roy, P., Orr, P.J., Botting, J.P., Muir, L.A., Vinther, J., Lefebvre, B., El Hariri, K., and Briggs, D.E., 2010, Ordovician faunas of Burgess Shale type: Nature, v. 465, p. 215–218, https://doi.org/10.1038/nature09038.

Van Roy, P., Briggs, D.E.G., and Gaines, R.R., 2015, The Fezouata fossils of Morocco; an extraordinary record of marine life in the Early Ordovician: Journal of the Geological Society, v. 172, p. 541–549, https://doi.org/10.1144/jgs2015-017.

Vaucher, R., Martin, E.L.O., Hormière, H., and Pittet, B., 2016, A genetic link between Konzentrat and Konservat Lagerstätten in the Fezouata Shale (Lower Ordovician, Morocco): Palaeogeography, Palaeoclimatology, Palaeoecology, v. 460, p. 24–34, https://doi.org/10.1016/j.palaeo.2016.05.020.

Vaucher, R., Pittet, B., Hormière, H., Martin, E.L.O., and Lefebvre, B., 2017, A wave-dominated, tide-modulated model for the lower Ordovician of the anti-atlas, Morocco: Sedimentology, v. 64, p. 777–807, https://doi.org/10.1111/sed.12327.

Vorhies, J.S., and Gaines, R.R., 2009, Microbial dissolution of clay minerals as a source of iron and silica in marine sediments: Nature Geoscience, v. 2, p. 221–225, https://doi.org/10.1038/ngeo441.

FIGURE CAPTIONS

Figure 1. Minerals identification in samples from the Fezouata Shale from X-ray powder diffraction. The box with red margins is an expansion of the area indicated in the main plot.

Figure 2. From left to right: sequences of various scales translating sea-level cycles at different timescales, part of the sedimentary succession of Fezouata Shale with location of samples, facies F1, F2 and F4 as described in Vaucher et al. (2017) used to identify the sequences, relative bathymetry changes and oxygen fluctuations.

Figure 3. Model explaining the effect of orbital forcing on seasonality, and thus on soft tissues preservation.

1GSA Data Repository item 2018xxx, xxxxxxxxxxxxxxxx, is available online at http://www.geosociety.org/datarepository/2018/, or on request from editing@geosociety.org.

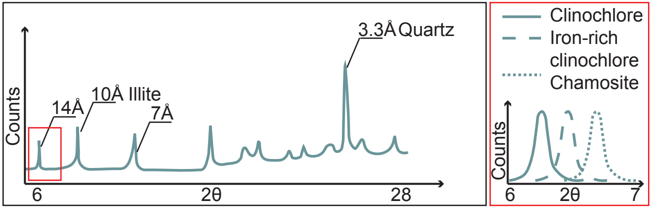

3.3Å Quartz
10Å Illite
14Å
7Å
Counts
6
2θ
28
Clinochlore
Iron-rich
clinochlore
Chamosite
Counts
6
2θ
7

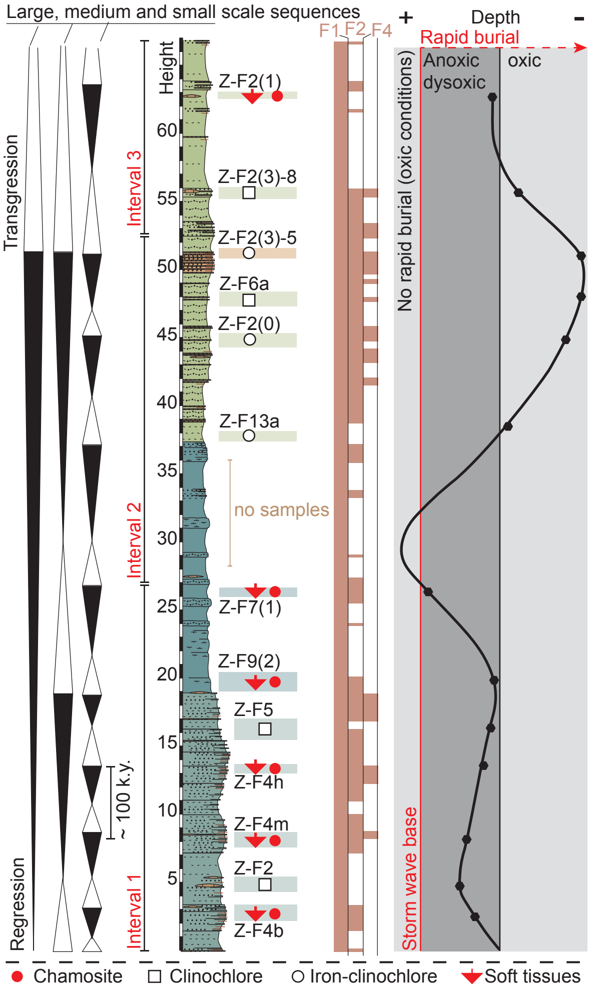

Large, medium and small scale sequences
Transgression
Regression
Height
Interval 3
Interval 2
Interval 1
~ 100 k.y.
Z-F2(1)
Z-F2(3)-8
Z-F2(3)-5
Z-F6a
Z-F2(0)
Z-F13a
no samples
Z-F7(1)
Z-F9(2)
Z-F5
Z-F4h
Z-F4m
Z-F2
Z-F4b
F1 F2 F4
+ Depth -
Rapid burial
No rapid burial (oxic conditions)
Anoxic dysoxic
oxic
Storm wave base
Chamosite
Clinochlore
Iron-clinochlore
Soft tissues

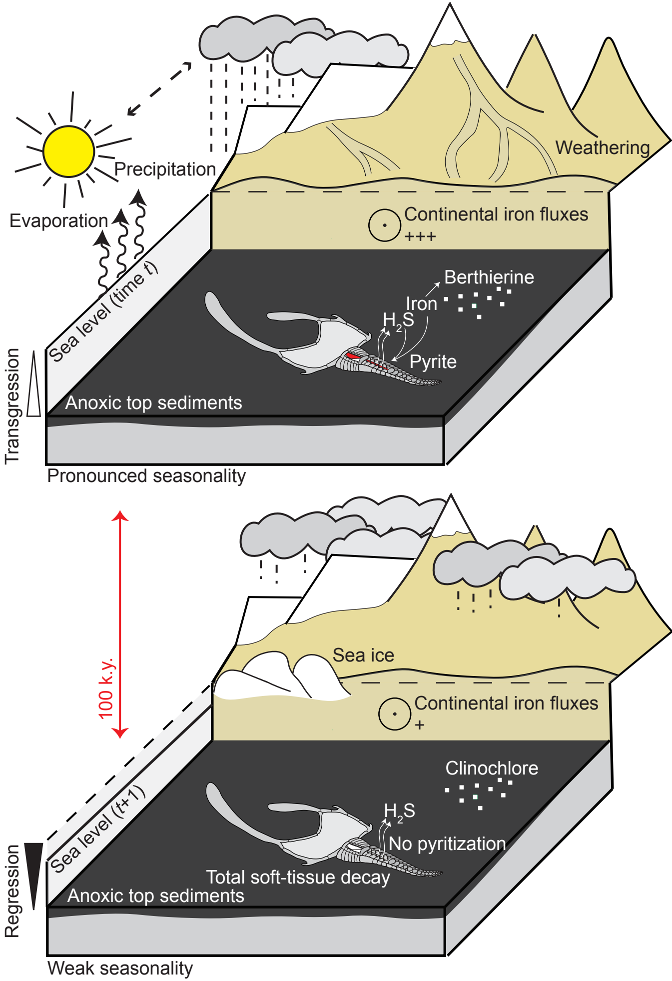

Precipitation
Evaporation
Weathering
Continental iron fluxes
+++
Berthierine
Iron
H_2S
Pyrite
Sea level (time *t*)
Transgression
Anoxic top sediments
Pronounced seasonality
100 k.y.
Sea ice
Continental iron fluxes
+
Clinochlore
H_2S
No pyritization
Total soft-tissue decay
Sea level (*t*+1)
Regression
Anoxic top sediments
Weak seasonality